Behavioral state modulates the ON visual motion pathway of *Drosophila*

James A. Strother[a,1,2], Shiuan-Tze Wu (吳宣澤)[a,1,3], Edward M. Rogers[a], Jessica L. M. Eliason[a], Allan M. Wong[a], Aljoscha Nern[a], and Michael B. Reiser[a,4]

[a]Janelia Research Campus, Howard Hughes Medical Institute, Ashburn, VA 20147

Edited by S. Lawrence Zipursky, University of California, Los Angeles, CA, and approved November 17, 2017 (received for review February 22, 2017)

The behavioral state of an animal can dynamically modulate visual processing. In flies, the behavioral state is known to alter the temporal tuning of neurons that carry visual motion information into the central brain. However, where this modulation occurs and how it tunes the properties of this neural circuit are not well understood. Here, we show that the behavioral state alters the baseline activity levels and the temporal tuning of the first directionally selective neuron in the ON motion pathway (T4) as well as its primary input neurons (Mi1, Tm3, Mi4, Mi9). These effects are especially prominent in the inhibitory neuron Mi4, and we show that central octopaminergic neurons provide input to Mi4 and increase its excitability. We further show that octopamine neurons are required for sustained behavioral responses to fast-moving, but not slow-moving, visual stimuli in walking flies. These results indicate that behavioral-state modulation acts directly on the inputs to the directionally selective neurons and supports efficient neural coding of motion stimuli.

motion vision | behavioral-state modulation | *Drosophila*

The neuronal processing in visual systems has traditionally been understood using static feedforward models, but recent work has shown that in many animals these neural circuits are not stationary but are instead substantially altered by the animal's behavioral state (1–4). Flies have long been used to study visually guided behaviors and the neuronal circuits implementing visual processing, and flies have also recently emerged as a model system for understanding how the behavioral state of an animal might affect these circuits. Much of this research has focused on the neural circuits that provide visual estimates of motion, which flies—like many animals—rely on to navigate through their environment. The strongest evidence for behavioral-state modulation of motion detection comes from recordings of lobula plate tangential cells (LPTCs), a family of giant neurons that project from the optic lobe to the central brain. Many LPTCs encode patterns of visual motion that correspond to canonical modes of rotational self-movement (e.g., roll, pitch, yaw), by integrating locally oriented, directionally selective inputs over a large receptive field (5). Several LPTC types show enhanced responses to motion in the preferred direction when the animal is in flight compared with when it is not flying [VS cells (3, 6); H1 cells (7)]. Such findings have also been applied to explain the significant differences between behavioral assays and physiological measurements from quiescent animals in the temporal tuning of responses to visual motion (1, 7).

The effects of behavioral state appear to be principally the result of neuromodulation mediated by octopamine, an invertebrate transmitter that is closely related to norepinephrine (8). In crickets, octopamine levels in the hemolymph are elevated following periods of increased behavioral activity, including aggressive interactions, courtship, and flight (9). In flies, octopamine neurons increase activity during transitions from quiescence to an active behavioral state (6). Furthermore, bath application of octopamine or chlordimeform (CDM), an octopamine agonist, produces many of the same changes in neuronal responses that are observed during periods of increased behavioral activity (2, 6, 7, 10–12). In addition, silencing of octopamine neurons removes many of the effects of behavioral state on LPTC responses (6) and reduces the behavioral responses of flying flies to fast, but not slow, visual stimuli (13). Nonetheless, the precise mechanism by which the behavioral state of the animal and octopamine neuromodulation alter the dynamics of the insect visual system remains unclear, and so this study is focused on addressing this gap. Although several studies have examined the LPTCs at the output of the visual system, octopamine neurons project broadly throughout the optic lobes (14), and it is likely that neurons well upstream of the LPTCs are modulated by behavioral state. Indeed, similar behavioral and octopamine modulation of response amplitude and temporal tuning has been observed in the Lawf2 neurons of the medulla, which are wide-field neurons that encode luminance but not motion changes (12). However, outside of the LPTCs and Lawf2 neurons, the scope of octopaminergic modulation in the visual system is unknown.

Examinations of behavioral-state modulation are aided by recent studies that have provided a basic outline of the neural circuits that detect visual motion. As currently understood, the core of the motion pathway is a primarily feedforward circuit composed of neurons from the retina, lamina, medulla, lobula, and lobula plate. Photoreceptors of the retina synapse onto the columnar

Significance

Animal visual systems are typically thought of by analogy to cameras—sensory systems providing continuous information streams that are processed through fixed algorithms. However, studies in flies and mice have shown that visual neurons are dynamically and adaptively retuned by the behavioral state of the animal. In *Drosophila*, prominent higher-order neurons in the visual system respond more strongly to fast-moving stimuli once the animal starts walking or flying. In this study, we systematically investigated the neurobiological mechanism governing the behavioral-state modulation of directionally selective neurons in *Drosophila*. We show that behavioral activity modifies the physiological properties of critical neurons in this visual motion circuit and that neuromodulation by central feedback neurons recapitulates these effects.

Author contributions: J.A.S., S.-T.W., A.M.W., and M.B.R. designed research; J.A.S., S.-T.W., E.M.R., J.L.M.E., and A.M.W. performed research; J.A.S. and A.N. contributed new reagents/analytic tools; J.A.S., S.-T.W., and J.L.M.E. analyzed data; and J.A.S., S.-T.W., and M.B.R. wrote the paper.

The authors declare no conflict of interest.

This article is a PNAS Direct Submission.

Data deposition: All data, reagents, and code used in this manuscript will be provided upon request by M.B.R. (reiserm@janelia.hhmi.org).

[1]J.A.S. and S.-T.W. contributed equally to this work.

[2]Present address: Department of Integrative Biology, Oregon State University, Corvallis, OR 97331.

[3]Present address: Division of Biological Sciences, University of California, San Diego, CA 92122.

[4]To whom correspondence should be addressed. Email: reiserm@janelia.hhmi.org.

This article contains supporting information online at www.pnas.org/lookup/suppl/doi:10.1073/pnas.1703090115/-/DCSupplemental.

lamina neurons (second-order interneurons), which synapse principally onto columnar medulla neurons (third order), which synapse onto columnar neurons with dendrites in the medulla (T4) and the lobula (T5); these fourth-order cells then synapse onto the LPTCs of the lobula plate (fifth order), which project into the central brain (15–17). Although the inputs (the photoreceptors and lamina neurons) and the outputs to this circuit encode both ON (luminance increases) and OFF (luminance decreases) signals, the intermediate computations are performed by functionally independent pathways that are selective for either ON or OFF stimuli (18–22). In each of these pathways, the columnar medulla neurons encode nondirectionally selective luminance information that is integrated by T4 or T5 cells (ON and OFF, respectively) to produce a directionally selective signal (each cell type has four subtypes selective for each cardinal direction) (18, 23–25). Consequently, the outputs of T4 and T5 appear to represent the outputs of elementary motion detectors (EMDs) that compute a local motion signal for each ommatidium of the eye, consistent with previous behavioral studies (26).

In this study, we have focused on the neurons of the ON motion pathway. We examined the directionally selective T4 cells, and each of their primary inputs, the columnar neurons Mi1, Tm3, Mi4, and Mi9 (17, 23, 27) (Fig. 1*A*). In previous work, we used two-photon imaging to characterize the responses of Mi1, Tm3, Mi4, and Mi9 to visual stimuli. We showed that these neurons are not directionally selective, while the dendrites of T4 neurons are directionally selective (23), indicating that this selectivity emerges in the dendrites of T4 cells [mirroring recent results in the OFF pathway (24, 25)]. Furthermore, silencing experiments suggest that Mi1 and Tm3 are the dominant excitatory inputs for T4 cells, and functional connectivity studies suggest that these two inputs act synergistically to produce the directional selectivity of T4 cells (23). The same study indicated that Mi4 and Mi9 neurons provide inhibitory inputs to T4 that are not necessary for the directional selectivity of T4 cells, but do shape its temporal tuning. These results suggest that the directional selectivity of T4 cells emerges through a nonlinear integration of Mi1 and Tm3 inputs, while inhibitory inputs from Mi4 and Mi9 further tune the computation. However, although these results do suggest a role for Mi4 and Mi9 neurons, the exact nature of their contribution to this circuit remains unclear. This is especially true for Mi4 neurons. Paradoxically, silencing experiments indicate that blocking the synaptic transmission of Mi4 neurons does alter the behavioral turning response but does not affect the response of T4 cells to motion stimuli as measured using calcium imaging in quiescent animals (23). We interpreted these results as potential evidence that the behavioral state of the animal strongly affects the function of this circuit.

In this study, we asked whether the fly's behavioral state modulates the neurons of the ON motion pathway. While it is now widely accepted that the behavioral state affects the speed tuning of fly visual motion estimation, where and how this modulation occur have remained open questions. We show here that octopamine neurons are required for sustained behavioral responses to fast visual motion in walking animals. We further show that, for each of the major neurons in the ON motion pathway, the responses to fast motion stimuli are enhanced during the active behavioral state and through octopamine modulation. We also examine the physiological basis for these changes and demonstrate that octopaminergic input modulates the excitability of one of T4's major input neurons. These results strongly suggest that behavioral-state modulation acts very early in this pathway before the emergence of directional selectivity and that the observed speed tuning changes are at least in part a consequence of changes in the excitability of medulla interneurons. These findings reveal both the location and a key mechanism of behavioral-state modulation in the ON motion pathway of *Drosophila*.

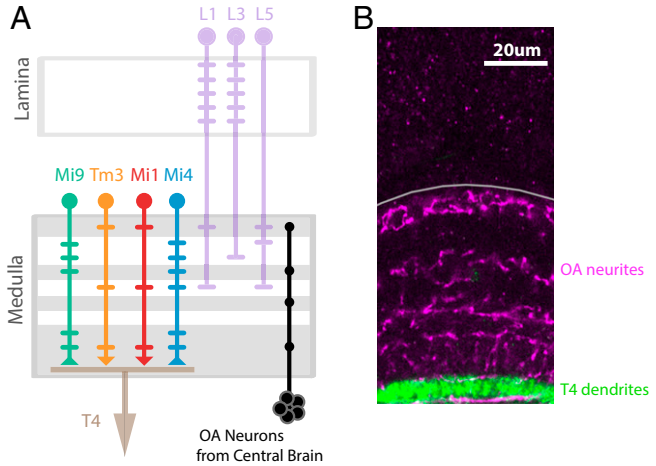

Fig. 1. Directional selectivity first emerges in the fly medulla, which is also densely innervated by octopamine neurons. (*A*) Schematic model of the early fly visual system, depicting the columnar neuron types that make up the ON motion circuit. Directional selectivity is synthesized in the dendrites of T4 cells from inputs conveyed by the nonselective neurons Mi9, Tm3, Mi1, and Mi4 (23). These T4 input neurons in turn receive major inputs from three types of lamina monopolar cells (L1, L3, L5). Only one example of each columnar cell type is shown here, but neurons of each type are present in every column of the visual system. The horizontal bars extending from each neuron's axon indicate the location of fine branches and synaptic contacts. The excitatory synaptic inputs from Tm3 and Mi1 onto T4 are indicated with a downward arrowhead, while the inhibitory inputs from Mi9 and Mi4 onto T4 are indicated by an upturned arrowhead (signs are based on ref. 23; the relative spatial offsets between the cell types are based on ref. 27). The octopamine (OA) neurons project from the posterior slope of the central brain into the medulla (14); innervation layers of the octopamine cells are indicated with gray horizontal bars. (*B*) The expression pattern of octopamine neurons (magenta) and T4 cells (green) in the fly medulla (outlined in gray; genotype in Table S1). The octopamine neurons do not project into the lamina, and so octopamine modulation of the ON motion pathway is expected to occur downstream of the lamina.

Results

The Activity of ON Motion Pathway Neurons Correlates with Behavioral State. To determine whether the properties of the ON motion pathway are modulated by the behavioral state of the animal, we first examined whether the activity of the major neurons in this pathway (Mi1, Tm3, Mi4, Mi9, and the directionally selective T4; Fig. 1) are affected by spontaneous changes in the behavior of the animal. Each of these cell types was targeted either using a split-GAL4 driver line (28, 29) or a lexA line (29, 30) identified in a previous study (23), or by surveying a large collection of imaged driver lines (29, 31). These genetic driver lines were used to express a genetically encoded fluorescent calcium indicator [GCaMP6f for Mi1, Tm3, Mi4, and Mi9; GCaMP6m for T4 (32)]. Detailed genotypes for all of the experimental animals used throughout this study are provided in Table S1. The flies were tethered to a perfusion chamber, and the cuticle at the back of the head was removed to provide optical access to the visual system. In vivo two-photon microscopy was used to record the fluorescence of the calcium indicator in the medulla while the animals were maintained in a dark environment. The calcium activity ($\Delta F/F$) was calculated as the difference between the instantaneous and baseline fluorescence normalized by the baseline fluorescence (taken as the 10% quantile over the entire recording period). Flies in such a preparation will remain quiescent for short periods of time (tens of seconds), interrupted by bouts of spontaneous leg movement and other observable behavioral activity. The spontaneous leg movements of the fly were recorded using an infrared-sensitive camera positioned underneath the tethered animal that was illuminated with near-infrared light. A dimensionless "movement index" was calculated from movies of leg movements, based

on the time derivative of the pixel intensities for a manually selected region of interest around the legs (*Materials and Methods*). The time series recorded from these experiments suggested that spontaneous behavioral activity correlated with changes in baseline calcium activity for several of the cell types (examples of typical data in Fig. 2*A*). In particular, Mi4 cells showed remarkable swings in baseline activity that were highly correlated with spontaneous leg movements (Movie S1). To examine this relationship further, we calculated the linear convolution kernel that best predicted the measured calcium activity using the movement index as input (Fig. 2*B*). The convolution kernel for Mi1 neurons took the form of a ∼1-s-long positive bump centered at time 0, indicating that calcium activity of Mi1 cells was positively correlated with the leg movement and that this increase in calcium activity neither substantially preceded nor lagged behind the leg movement. The convolution kernel computed for Tm3 cells had a similar shape but a negative sign, indicating that the Tm3 calcium activity decreased during periods of spontaneous leg movements. Consistent with our observations from the individual time series, the convolution kernel computed for Mi4 cells had a similar form to the kernels observed for other neurons but was notably larger in magnitude (especially when the response is normalized by the response to other stimuli; Fig. S1*A*). This further demonstrates that the activity of Mi4 cells increased dramatically during periods of spontaneous leg movement. In contrast, there was no statistically significant relationship between calcium activity and spontaneous leg movement in either Mi9 or T4 cells.

The correlation between the calcium activity of neurons in the ON pathway and spontaneous leg movements suggested that several of these neuron types are modulated by the behavioral state of the animal. To test this directly, we examined whether induced changes in the behavioral state would produce similar changes in the calcium activity. A small tube was positioned underneath the tethered fly, and a series of air puffs was delivered to the animal. Air puffs are known to induce flight in tethered *Drosophila* (33). Although in our setup the flies were tethered in such a way that they would not fly continuously, these air puffs reliably induced short bouts of behavioral activity. The animals were kept in a darkened arena, the calcium activity of neurons and leg movements were measured simultaneously, and air puffs were delivered to the animal at 30-s intervals. The recorded time series suggest that, as expected, the air puffs elicit a shift in the behavioral state as evidenced by periods of intensive leg movements (Fig. 2*C* and Movie S1). To examine the effects of these induced changes in behavioral state, we calculated the stimulus-aligned calcium response of each of the cell types to an air puff and found statistically significant responses for all five cell types. In Mi1, Mi9, and T4 cells, air puffs produced an increase in calcium activity that lasted for ∼1 s (Fig. 2*D*). Interestingly, air puffs produced a transient response in Tm3 cells. In these cells, the air puff elicited a brief decrease in calcium activity, which was then followed by a sustained period of increased calcium activity. However, consistent with our previous findings, Mi4 cells showed the most pronounced response to air puffs. In these cells, an air puff produced a substantial increase in calcium activity that was sustained for several seconds. Although the baseline shift observed in Mi4 was exceptionally large, the responses of Mi1, Tm3, Mi9, and T4 were substantial in their own right and had peak $\Delta F/F$ values that were ∼10–30% of the maximum $\Delta F/F$ observed in response to moving grating visual stimuli (see Fig. 4*C*). These results are principally consistent with the convolution kernels observed in response to spontaneous leg movements, although the responses of Mi9 and T4 cells did not rise to statistical significance when examining spontaneous behavioral activity.

Together, these results suggest the physiological properties of these neurons are strongly modulated by the behavioral state of the animal. In particular, Mi4 cells appear exceptionally sensitive to the behavioral state and demonstrate a very high baseline activity during periods of behavioral activity while maintaining a low baseline activity during periods of behavioral quiescence.

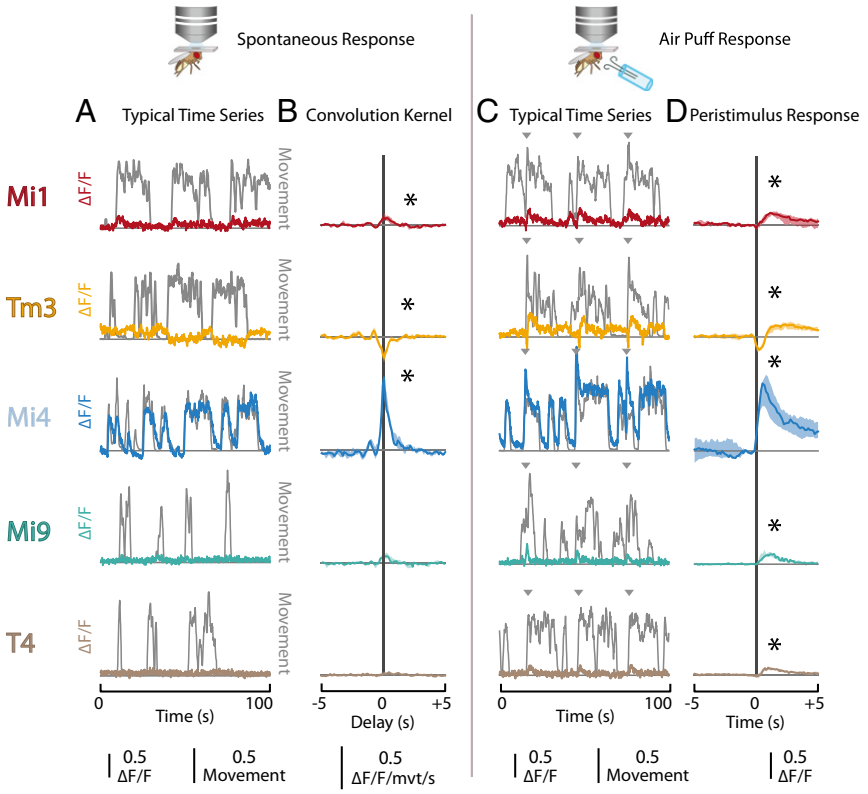

Fig. 2. Behavioral state modulates baseline activity of neurons in the ON pathway. (*A* and *B*) Flies were mounted to a perfusion chamber in a darkened arena. The spontaneous leg movements were then recorded while the activity of neurons in the ON pathway was simultaneously measured using a fluorescent calcium indicator (GCaMP6f or GCaMP6m). The activity of the neuron types Mi1, Tm3, Mi4, Mi9, and T4 are shown in rows. (*A*) A typical time series showing the activity of the neuron type in color and the dimensionless movement index in dark gray. (*B*) The linear convolution kernel that best predicts the activity of the neuron type from the movement index. Results are the median values (error bars are 25–75% quantiles) from multiple individuals ($n = 5$ for each genotype). Asterisks indicate kernels in which the mean for the −1- to 1-s interval is significantly different from zero (two-tailed t test, $P < 0.05$). (*C* and *D*) A series of air puffs were delivered to the animal in a darkened arena at 30-s intervals, and the activity of neuron types in the ON pathway and the leg movements of the animal were simultaneously recorded. As in *A* and *B*, the activity of the different neuron types is presented in rows. (*C*) A typical time series showing the activity of the neuron type in color, movement index in gray, and time of air puffs as gray arrowheads. (*D*) Stimulus-aligned calcium response of each neuron type. Results are the median values (error bars are 25–75% quantiles) from multiple individuals ($n = 5$ for each genotype). Asterisks indicate responses in which the mean for the 0- to 1-s interval is significantly different from zero (two-tailed t test, $P < 0.05$). The five genotypes used in these results are detailed in Table S1.

Similar baseline shifts in the membrane potential of the downstream LPTCs have been observed in flies in the dark during periods of active walking (34) or flying (35). Interestingly, T4 neurons that are downstream of Mi4 neurons and upstream of LPTCs do not show such pronounced increases in baseline activity. This may suggest that the baseline shifts in the LPTCs are a result of inputs from other neurons, such as T5 cells (36). While T4 neurons receive a mixture of inhibitory and excitatory inputs that are both affected by the behavioral state, all known columnar inputs to T5 cells are probably excitatory (25, 37). An increase in the strength of any excitatory T5 inputs during the active behavioral state would be expected to produce a baseline shift in T5 and consequently the LPTCs.

Furthermore, although the effects of spontaneous behavioral activity and air puffs were similar across the cell types investigated in this study, the differences may prove informative. For example, although spontaneous behavioral activity and air puffs were both associated with transient decreases in the calcium activity of Tm3 cells, only in response to air puffs was this decrease followed by a period of sustained, increased calcium activity. Such differences suggest that behavioral-state modulation of the visual system is not simply present or absent, but rather has multiple dimensions with characteristic effects on different cell types.

Octopamine Neurons Are Necessary for Sustained Turning Responses to Fast Motion Stimuli in Walking Flies. Octopamine neurons have been shown to modulate optic lobe neurons during flight (6, 13). Given the effects of spontaneous leg movement on the baseline activity of medulla interneurons (Fig. 2 *A* and *B*), we next examined whether octopamine neurons also modulate visual function in the walking behavioral state. We silenced octopamine neurons by expressing the Kir2.1 potassium channel using the Tdc2-GAL4 (38) driver (Fig. 3*A*). Flies were then tethered and allowed to walk on an air-supported ball setup that recorded their walking speed and heading (39), while visual motion stimuli were presented on an LED display (40) (Fig. 3*B*).

When presented with a rotating visual motion stimulus, walking flies turn in the direction of motion with an amplitude that depends on the speed of the motion stimulus (19, 23). We found that, for short visual motion presentations (0.25 and 0.5 s; *Top* two rows of Fig. 3*C*), flies with silenced octopamine neurons had turning responses similar to control flies for most grating speeds and only showed significantly reduced responses to the two fastest stimuli (16- and 24-Hz grating temporal frequency, or 480°/s and 720°/s). However, when the duration of the stimulus presentation was increased (2 and 4 s; *Bottom* rows of Fig. 3*C*), flies with silenced octopamine neurons showed reduced response to all gratings with a temporal frequency greater than 8 Hz. Importantly, the turning differences between control flies and those with silenced

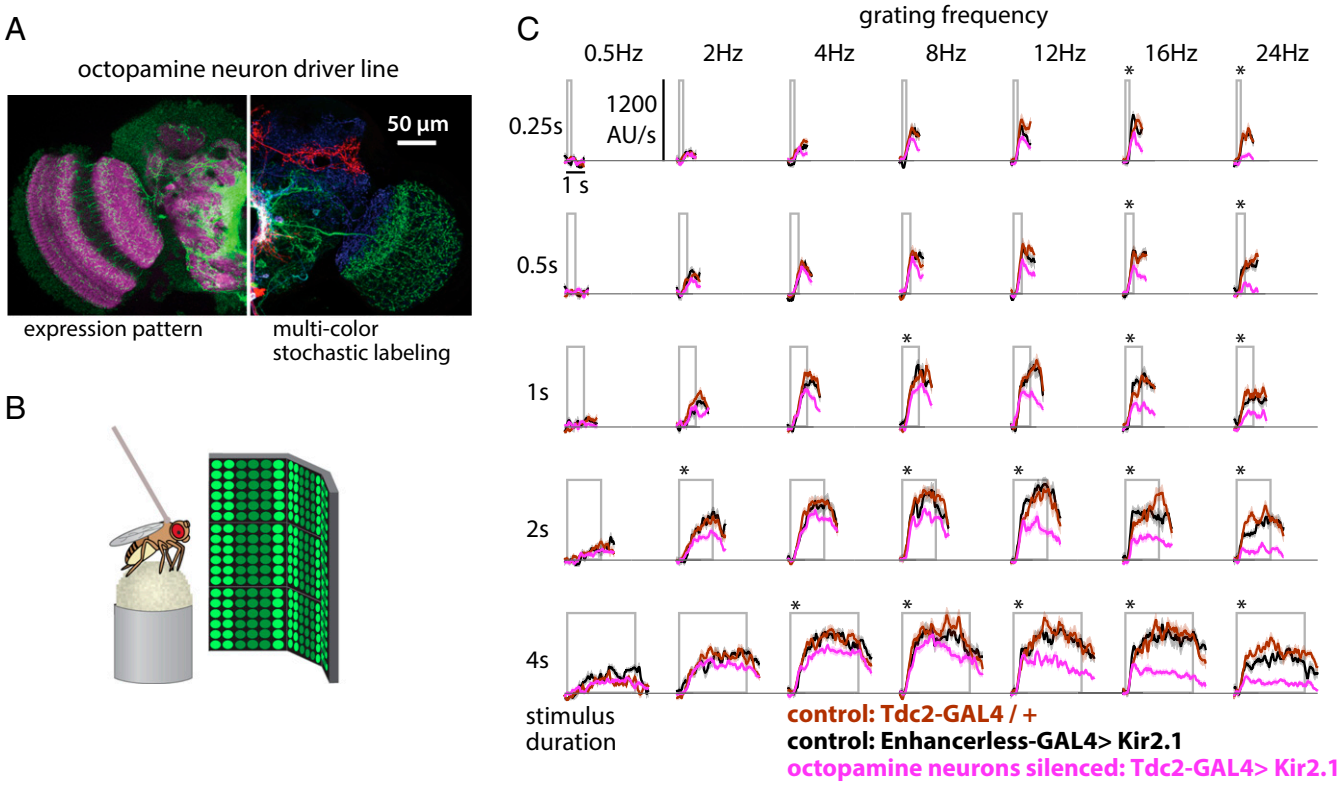

Fig. 3. Octopamine neurons are required for sustained behavioral responses to fast visual motion stimuli in walking flies. (*A*) Octopamine neurons were targeted using the Tdc2-GAL4 line. For silencing experiments, we expressed a GFP-tagged Kir2.1 channel in the octopamine neurons and confirmed the expression pattern of this effector. *Left* side shows a single image plane from a confocal stack of the whole expression pattern (anti-GFP staining). The *Right* side shows the maximum intensity projection of a stochastic labeling method [Multicolor FlpOut (57)] that reveals the morphology of individual octopamine neurons, including two distinct cell types that project into the optic lobe. (*B*) Schematic representation of the apparatus used to measure the turning reactions of tethered flies walking on an air-supported ball. The complete visual display covered 270° in azimuth of the fly's field of view and was used to present grating patterns (23% contrast and 30° spatial period) moving at different speeds. (*C*) Fly turning responses to the presentation of rotational grating motion at different speeds (indicated by the grating frequency) and different stimulus durations. The magenta lines represent the behavioral responses of flies with silenced octopamine neurons, while the black and brown lines represent the responses of control genotypes. The gray box represents the period of stimulus movement. Results shown are the median values (±SEM) from multiple flies (n = 10 individuals for all genotypes). Asterisks indicate responses where the mean response differs significantly from both control lines (t test controlled for false discovery rate, $P < 0.05$).

octopamine neurons only emerged after hundreds of milliseconds, suggesting that octopamine neurons may contribute to the maintenance of responses to faster visual motion. It is unclear whether this result is specific to walking, as similar effects have not been observed when octopamine neurons were silenced in flying animals (6, 13). Intriguingly, electrophysiological recordings from the LPTCs indicate that these neurons show more sustained responses to moving visual stimuli when the animals are flying than when they are behaviorally quiescent (36). The forward walking velocity in flies with silenced octopamine neurons is not clearly reduced in comparison with control flies during these visual stimuli, but silencing octopamine neurons appears to reduce the modulation of forward walking velocity (Fig. S2). Octopamine could also alter behavior by acting on neurons downstream of T4 or nonnervous tissues, such as muscles, or after circulating through the hemolymph. While we cannot rule out a nonvisual or nonnervous contribution of octopamine neuromodulation to the behavioral consequence of silencing octopamine neurons, the specific reduction in sustained turning reactions to fast visual motion (and not just large turning reactions) strongly argues for a role of octopamine release in the visual system contributing to speed tuning of the motion pathway. Nevertheless, the interactions of neuronal adaptation, temporal integration of neuronal responses, and nonnervous octopamine effects are interesting areas for future investigation.

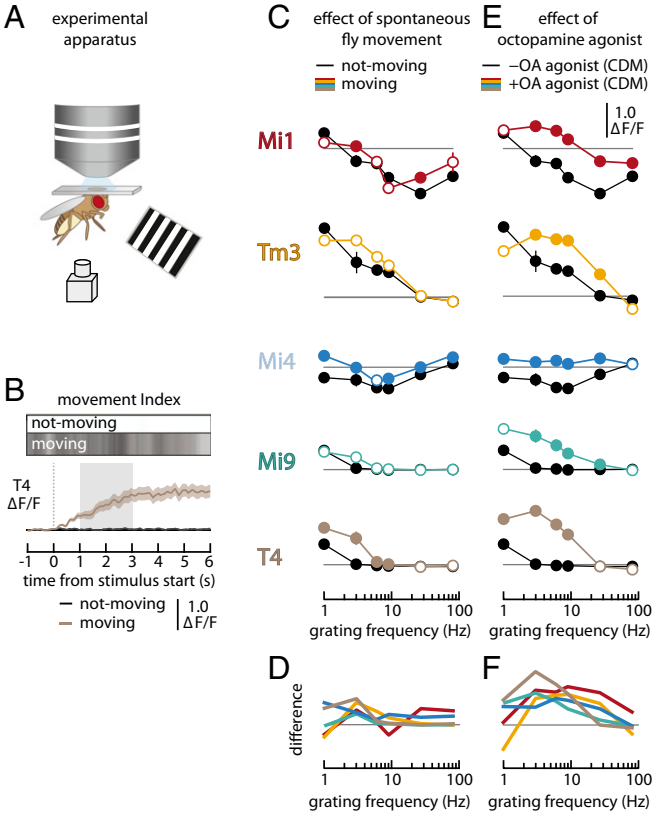

Fig. 4. Behavioral state modulates the frequency tuning of all ON pathway neurons examined. (*A*) Schematic of the experimental setup where flies were presented with moving grating stimuli while the calcium activity of neurons in the medulla was imaged and spontaneous leg movements were recorded. (*B*) Calcium response of T4 neurons (from $n = 5$ individuals, pooled and presented as median ± SEM) to the presentation of a moving-grating stimulus (3 Hz, 100% contrast, anterior-to-posterior). Results are shown during periods of behavioral quiescence (black line near zero, not-moving) and during periods of spontaneous activity (brown line, moving). The grayscale bars above the plot show the movement index as a function of time for both conditions (white = 0; black = 1). The dashed vertical line indicates the start of the stimulus, and the shaded area represents the time period from which responses were averaged to produce the tuning curves in *C* and *E*. Time series for other cell types are presented in Fig. S1C. (*C*) Tuning curves for the calcium response of several neuron types (in rows, genotypes detailed in Table S1) to a moving grating. Each stimulus was presented to each individual six times, and the responses were sorted into not-moving (black lines) and moving (colored lines) groups based on the spontaneous movement of the animal during the stimulus period. The responses from $n = 5$ individuals (for each genotype) were pooled and are presented as median ± SEM. Filled circles indicate stimuli for which the moving responses are significantly different from the not-moving values (*t* test controlled for false discovery rate, $P < 0.05$). The not-moving responses are shown as filled circles, although this does not represent any statistical test. (*D*) Tuning curves showing the difference between the moving and not-moving conditions. Data are replotted from and lines are colored as in *C*. (*E*) Tuning curves for the calcium response of several neuron types (in rows) to a moving grating after the addition of the octopamine agonist CDM to the saline bath. The responses in the presence of CDM (10 μM; colored lines) were measured from $n = 5$ individuals (for each genotype) and pooled without sorting for leg movement during the stimulus. These are compared with the responses measured in not-moving animals in the absence of CDM (from *A*, black lines). Results are shown as in *C*. (*F*) Tuning curves showing the difference between CDM and CDM-free conditions. Data are replotted from and lines are colored as in *E*.

The Behavioral State Alters the Frequency Response of ON Pathway Neurons. Our silencing experiments (Fig. 3*C*) showed that octopamine neurons, thought to modulate the visual system during active behavioral states, are necessary for turning responses to faster visual motion stimuli in walking flies. Similarly, several prior studies in *Drosophila* and other flies have found that the frequency tuning of LPTCs (1, 6, 7) and other neurons in the visual system (12) broadens to encode faster inputs when the animals are in an active behavioral state. We next asked whether the interneurons of the ON motion pathway (two synapses upstream of the LPTCs) show a similar shift in speed tuning with changes in the behavioral state. To examine this question, we added a projector-based visual display to our in vivo microscopy setup (Fig. 4*A*) and recorded the responses of each of the cell types to full-field gratings moving at different speeds (shown as the temporal frequency of the moving grating). Trials were sorted into "not-moving" and "moving" groups based on whether the flies displayed spontaneous leg movement during the grating stimulus period. For moving trials, we observed substantial enhancements in the response of neurons to higher-frequency gratings (T4 example shown in Fig. 4*B*; other cell types in Fig. S1*C*). Because the kinetics of GCaMP limits our ability to observe instantaneous fluctuations in calcium concentration, the response to a moving grating was quantified as the time-averaged fluorescence during the grating presentation (less the time-averaged fluorescence during the interstimulus interval, normalized by the baseline fluorescence). Increases in these time-averaged values with stimulus frequency reflect either increases in the amplitude of the neuron's response or positive baseline shifts. Tuning curves constructed from time-averaged values are minimally affected by the kinetics of the calcium indicator and have some favorable theoretical properties [see supplemental information in Strother et al. (22)].

Each cell type yielded a unique and characteristic tuning curve (nonmoving response curves in black; Fig. 4*C* and Fig. S1*C*). When flies were not moving, Mi1 cells responded to slow gratings (1 Hz) with an increase in time-averaged activity but responded to faster gratings (9–27 Hz) with a decrease in time-averaged activity. Tm3, Mi9, and T4 cells showed increased activity in response to all gratings, but the magnitude of this response decreased monotonically with increasing frequency. Mi4 cells responded to slow-moving gratings with a decrease in the time-averaged activity, which was most pronounced for fast-moving gratings (~9 Hz). When the fly was moving during the stimulus period, Mi1, Tm3, Mi9, and T4 cells all showed greater activity at higher frequencies compared with when the animal was not moving, although statistically significant differences (filled circles) were detectable only in Mi1 and T4 cells. In contrast, when the fly was moving during

the stimulus period, the tuning curve measured for Mi4 was shifted upward. The cumulative effect of spontaneous behavioral activity on the function of the visual system can be seen from the difference between the moving and not-moving tuning curves (Fig. 4*D*). Across the examined neurons, spontaneous activity yielded enhanced responses (all statistically significant differences were positive) and most of these enhancements occurred at frequencies between 1 and 10 Hz.

The effects of spontaneous behavioral activity on the responses of the neurons of the ON pathway suggest that the frequency tuning of these neurons is affected by the behavioral state of the animal. However, attempting to identify the specific effects of such behavioral-state modulation using spontaneous changes in the behavioral state is substantially complicated by uncertainty in assessing the exact behavioral state of the animal at the time of the measurement, the possibility that the visual stimulus itself can elicit changes in the behavioral state of the animal, and the logistical difficulty of adequately sampling the different behavioral states when they are not experimentally controlled. As such, we next examined the effects of a pharmacological treatment that effectively "clamps" the visual system in an "active" behavioral state. We measured the frequency tuning of each of the neurons in the ON motion pathway in the presence of 10 μM CDM, an octopamine agonist, and compared these responses with the frequency tuning observed for quiescent flies in the absence of CDM (Fig. 4*E* and Fig. S1*D*). In the presence of CDM, Mi1, Tm3, Mi9, and T4 cells showed greater activity at higher stimulus frequencies, consistent with our results for spontaneous changes in behavioral state. For example, the T4 cells in a quiescent animal show a very small response to a 3-Hz grating, while the T4 cells in a CDM-treated animal respond strongly to the same stimulus. Similarly, for a 9-Hz grating, Mi1 neurons showed decreased activity in the absence of CDM but increased activity in the presence of CDM. This change of sign could suggest that CDM increases the excitability of Mi1 neurons, or it might reduce the strength of inhibitory inputs tuned to high-frequency visual stimuli. The effect of CDM treatment on the responses of Mi4 cells was quite different from that of the other cell types. Mi4 cells responded to the moving-grating presentation with a decrease in calcium activity in the absence of CDM and a slight increase in activity in the presence of CDM. The net effect of CDM treatment on the visual system is illustrated by the difference between the CDM and control tuning curves (Fig. 4*F*). For each of the neurons, CDM treatment yielded enhanced responses (all statistically significant responses are positive), and for most neurons these differences had the form of a bandpass filter with a peak at ∼10 Hz. The sign of this effect is in agreement with a recent study that used white-noise stimuli to estimate the response kinetics of medulla neurons (41)—all temporal kernels become faster after application of CDM.

Although determining the baseline activity using nonratiometric calcium indicators such as GCaMP is challenging given the weak fluorescence levels at baseline and potential for photobleaching, for completeness we computed the baseline shift produced by application of CDM (Fig. S1*E*). Tm3 cells showed a small increase in baseline fluorescence, consistent with the air puff-induced baseline shift (Fig. 2) and the enhanced responses to moving gratings (Fig. 4*E*). The other cell types did not show a significant change in baseline activity, which may reflect the limited resolution of this approach or adaptation of the baseline activity.

It is interesting that, even in moving and CDM-treated flies, the speed tuning of T4 cells is slower than the speed tuning of the behavioral optomotor response (Fig. 4 *C–E* vs. Fig. 3*C*). Similar differences between the tuning of neurons in the motion vision pathway and behavioral responses have been observed in several previous studies (1, 2, 6, 7, 23). This difference could indicate that the flies in our walking assay are in a more active state than the flies in our imaging experiments, that octopamine modulation does not fully reproduce the behaviorally modulated neuronal state, or a combination of both factors. Alternatively, this might suggest that the behavioral response incorporates a parallel, possibly nondirectionally selective, pathway tuned to high-frequency visual stimuli.

Overall, these results suggest that the responses of Mi1, Tm3, Mi4, Mi9, and T4 cells to high-frequency stimuli are modulated by the behavioral state of the animal through an octopamine-dependent process. Our measurements cannot distinguish between differences in the time-averaged activity produced by changes in response amplitude vs. baseline shifts, which would be very interesting to pursue in future studies. Instead, our measurements indicate where modulation is occurring within the pathway and that the processing of faster visual stimuli is being affected. Although previous studies have shown that the directionally selective LPTCs downstream of the ON pathway are sensitive to both the behavioral state of the animal (3, 6, 7) and octopamine modulation (2, 6, 7, 10, 11), whether this modulation occurred at the LPTCs or upstream of the LPTCs has remained an open question. Silencing T4 and T5 cells has recently been shown to eliminate the behavioral-state signal measured in LPTCs (34). Our results push at least some of the behavioral-state modulation to even earlier stages of the visual system, and indicate that the directionally selective T4 neurons and LPTCs may simply inherit these effects from the neurons upstream of T4 (and presumably T5).

Stimulation of Octopamine Neurons Recapitulates Behavioral-State Changes in Medulla Interneurons of the ON Pathway. We have shown that the medulla interneurons that provide input to T4 neurons are modulated by both the behavioral state of the fly and an octopamine agonist. We next examined whether the shifts in activity we observed in the medulla interneurons in response to changes in behavioral state (Fig. 2) could be reproduced by depolarization of octopamine neurons. These experiments focused on the medulla interneuron that demonstrated the most remarkable behavioral-state modulation, Mi4, and an interneuron that showed fewer behavioral-state effects, Mi1 (Fig. 2).

We first used photoactivation experiments to identify the functional connectivity (42) between the same population of octopamine neurons examined in our behavioral assays and Mi4 neurons (Fig. 5 *A* and *B*). We reasoned that octopamine signaling onto Mi4 neurons may manifest as calcium increases, since several octopamine receptors are G-protein–coupled receptors that are known to increase intracellular calcium upon activation by octopamine (43, 44). These experiments require the use of two orthogonal genetic expression control systems. We used the GAL4/UAS system (45) to express the light-gated ion channel Chrimson (46) in the octopamine neurons labeled by Tdc2-GAL4 (38). We then simultaneously expressed the fluorescent calcium indicator GCaMP6s (32) in either Mi1 or Mi4 neurons (Fig. 5*C*) using the orthogonal LexA/LexAop system (30). Brains were excised and placed in physiological saline, and only brains with the laminas attached were used to ensure that the lamina monopolar cells remained intact. The Chrimson protein was activated using 660-nm light, and the fluorescence of GCaMP6s was recorded using two-photon microscopy (Fig. 5*B*).

Photoactivation of octopamine neurons produced a modest calcium response in the axons of Mi1 neurons. This response lagged behind the photoactivation period by several seconds, and the magnitude of this response was not strongly correlated with the photoactivation intensity (Fig. 5 *D–F*, *Left*). In contrast, photoactivation of octopamine neurons generated large calcium responses in the axons of Mi4 neurons, and these responses exhibited minimal lag and increased with increasing photoactivation intensity (Fig. 5 *D–F*, *Right*). These differences between Mi1 and Mi4 axonal responses were robust and were also measured in the dendrites (Fig. S3). These results largely mirror the modest Mi1 response and exceptionally large Mi4 response to spontaneous and induced changes in behavioral state (Fig. 2). These findings provide further evidence that behavioral-state

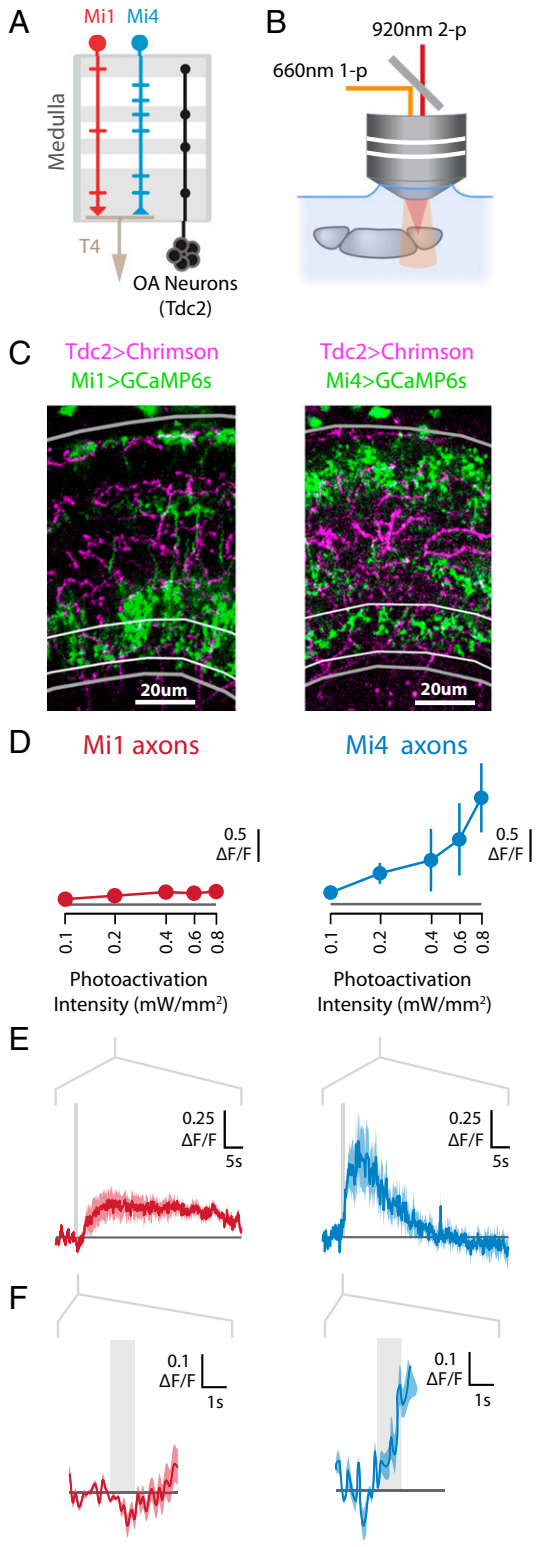

Fig. 5. The inhibitory medulla interneuron Mi4 is robustly and rapidly activated by stimulation of octopamine neurons. (*A*) Schematic model of the fly medulla, showing arborizations of Mi1, Mi4, T4, and octopamine (OA) neurons. Presented as in Fig. 1*A*. (*B*) Schematic diagram of experimental system used to examine functional connectivity between octopamine neurons and medulla interneurons. The light-gated channel protein Chrimson was expressed in the octopamine cell population (Tdc2-GAL4) and activated using a 660-nm light source, while the fluorescent calcium indicator GCaMP6s was expressed in either Mi1 or Mi4 and imaged using a two-photon microscope. (*C*) Expression patterns for Chrimson and GCaMP6s in the medulla for flies used in experiments described in *B*. Medulla cross-sections (4-μm slice; medulla outlined in gray; strata M10 outlined in white) show tdTomato-tagged Chrimson (magenta) in Tdc2-labeled neurons, and GCaMP6s (green) in Mi1 (*Left*) and Mi4 (*Right*) neurons (genotypes detailed in Table S1). (*D*) Tuning curves of axonal calcium responses (mean Δ*F*/*F* of strata M10) to a series of photoactivation pulses with increasing intensity. Data are shown as median ± SEM from multiple brains ($n = 6$ for Mi1 and Mi4). (*E*) Time series of axonal calcium responses (median ± SEM for $n = 6$) to photoactivation of the octopamine neurons (0.2 mW/mm^2 stimulation). The photoactivation period (1 s) is shown as a gray bar. The initial responses are replotted in *F*.

modulation acts via these octopamine neurons, and also suggest that Mi4 neurons are subject to especially substantial, likely direct, octopamine neuromodulation.

Octopamine Modulates the Excitability of Mi4. Since we had found that octopamine neurons are functionally connected to Mi4 neurons, we next asked whether this modulation also alters the excitability of Mi4 to its other synaptic inputs. Specifically, we examined whether octopaminergic neuromodulation changes the response of Mi4 cells to depolarization of one of its major inputs, the lamina monopolar cell L5 (Fig. 6*A*), using ex vivo photoactivation and imaging (Fig. 6*B*). Although the functional role of L5 neurons in motion vision is not well understood (47), EM reconstruction of the medulla has indicated that the L5 neurons are the predominant presynaptic partner to Mi4 cells (17).

We first confirmed that L5 neurons could be consistently depolarized using Chrimson. We coexpressed Chrimson and GCaMP6f in L5 neurons using a split-GAL4 driver line (47) (Fig. 6*C*) and then recorded the calcium response of L5 neurons to L5 photoactivation with and without the addition of the octopamine agonist CDM to the saline bath. A minimal concentration of CDM (50 nM) was used to minimize side effects on tyramine, dopamine, and serotonin receptors (48). We found that L5 neurons could be effectively depolarized using this approach. Photoactivation produced a rapid increase in calcium activity in L5 neurons, and increasing stimulus intensity yielded corresponding increases in the response magnitude (Fig. 6 *E* and *G*). Application of CDM did not have a statistically significant effect on these responses. Having established that L5 neurons could be consistently depolarized by Chrimson photoactivation and that these responses were largely unaffected by CDM, we next examined whether octopamine modulation altered the response of Mi4 neurons to depolarization of L5 neurons. We expressed Chrimson in L5 cells using the same split-GAL4 driver line and GCaMP6s in Mi4 cells using the orthogonal LexA/LexAop expression control system (Fig. 6*D*). We then recorded the response of Mi4 cells to depolarization of L5 neurons before and after the addition of CDM (50 nM) to the saline bath. We found that, in the absence of CDM, L5 photoactivation produces a modest increase in the calcium activity of Mi4 neurons and that the magnitude of this response saturates at high photoactivation intensities (Fig. 6*F*). However, in the presence of CDM, Mi4 neurons show much larger responses to L5 photoactivation, and these responses reach a greater asymptotic magnitude with increasing photoactivation intensity (Fig. 6 *F* and *H*). These findings were robust, and similar trends were observed in the dendrites of Mi4 neurons (Fig. S4*B*). Taken together, these results demonstrate that octopamine modulation substantially increases the excitability of Mi4 neurons to its synaptic inputs.

The recorded Mi4 responses had rather long decay times, returning to baseline values only after >10 s (Fig. 6*H*). These timescales are much longer than the temporal periods of the visual stimuli for which CDM had the greatest effect on the responses of the medulla neurons. However, the recorded responses are limited by the prolonged depolarization of L5 produced by Chrimson photoactivation and the slow speed of the calcium indicator

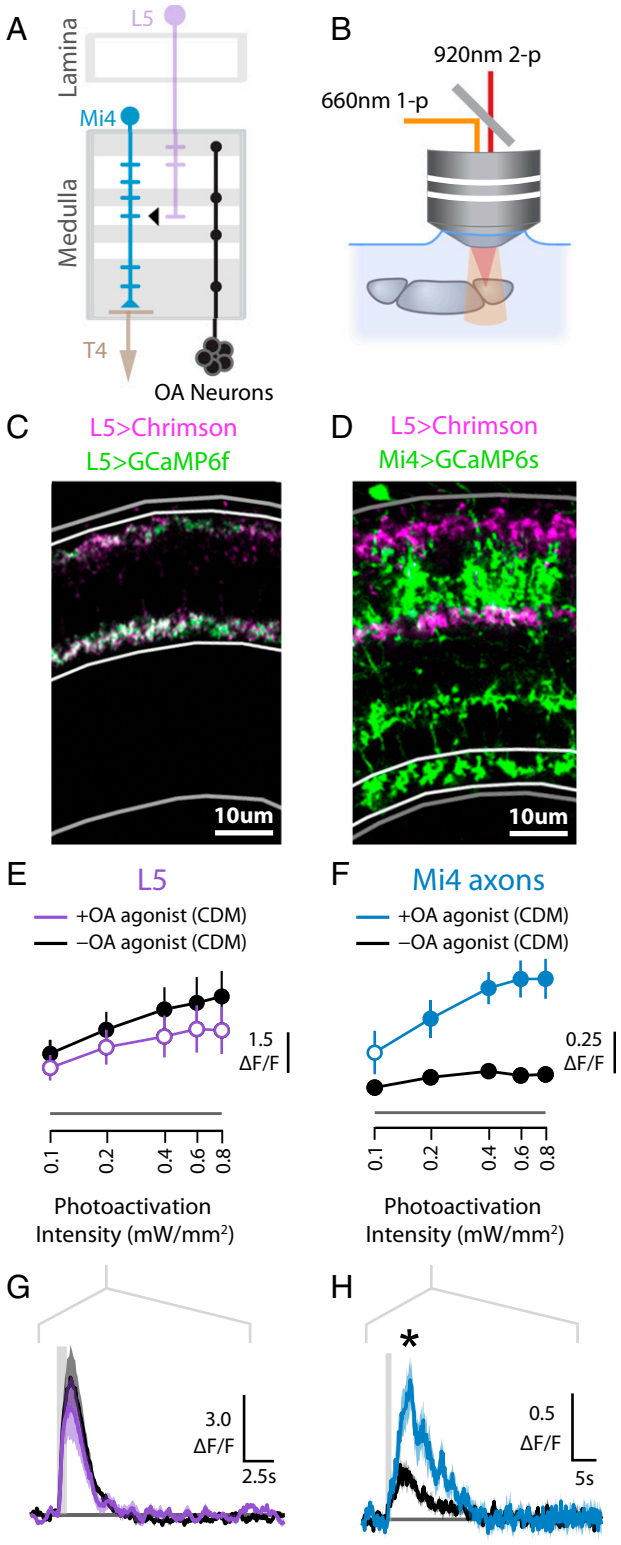

Fig. 6. Octopamine modulates the excitability of Mi4 neurons. (*A*) Schematic model of the lamina and medulla, showing arborizations of Mi4, L5, T4, and octopamine (OA) neurons. L5 neurons are a major presynaptic input to Mi4 neurons (17). (*B*) The experimental system used to examine functional connectivity. A 660-nm light source is used to activate the light-gated channel protein Chrimson. (*C*) Chrimson and GCaMP6f were expressed in L5 neurons. Medulla cross-sections (4-μm slice; medulla outlined in gray; strata M1–M5 outlined in white) show tdTomato-tagged Chrimson (magenta) and GCaMP6f (green) are colocalized in L5 neurons. (*D*) Medulla cross-sections (4-μm slice; strata M10 outlined in white) show tdTomato-tagged Chrimson (magenta) is expressed in L5 neurons and GCaMP6s (green) is expressed in Mi4 neurons. (*E*) Tuning curves of L5 calcium responses (mean Δ*F*/*F* of strata M1–M5) to L5 photoactivation. The colored line represents responses with the octopamine agonist CDM (50 nM), and the black line shows responses in the absence of CDM. For +CDM experiments, filled circles indicate responses that are significantly different from the control (*t* test controlled for false discovery rate, $P < 0.05$), which are shown with filled circles, although this does not represent any statistical test. Data are presented as median ± SEM Δ*F*/*F* from multiple brains ($n = 6$ for each +CDM and −CDM). (*F*) Tuning curves of Mi4 calcium response to L5 photoactivation. Data are presented as in *E*. (*G*) Time series (median ± SEM) of L5 calcium responses (Δ*F*/*F* of strata M1–M5) to L5 photoactivation (0.2 mW/mm^2). The photoactivation period (1 s) is indicated with a gray bar. (*H*) Time series of Mi4 calcium response (Δ*F*/*F* of strata M10) to L5 photoactivation (0.2 mW/mm^2), presented as in *G*. Asterisk indicates Mi4 response where CDM trial is significantly different from control.

GCaMP6s (32), and are thus unlikely to accurately capture the true kinetics of the Mi4 response. Similarly, CDM had only a small effect on the measured kinetics of the Mi4 response, although here too the slow kinetics of Chrimson and GCaMP6s may mask any such changes. Experiments using shorter photoactivation pulses and a faster calcium indicator (GCaMP6f) produced faster recorded Mi4 responses (Fig. S4*C*), although the duration of photoactivation and the speed of the calcium indicator are likely still limiting. Interestingly, high CDM concentrations appeared to push Mi4 neurons into an unresponsive physiological state (Fig. S4*D*), consistent with the conclusion that these neurons are exceptionally sensitive to octopamine neuromodulation and perhaps explaining the relatively weak Mi4 responses to moving-grating visual stimuli following CDM treatment (10 μM; Fig. 4*E*). However, it is difficult to compare the CDM concentrations between these experiments, since photoactivation was performed as an ex vivo experiment while the response to visual stimuli was measured through in vivo experiments, and the local CDM concentration may vary between these two preparations.

Discussion

The insect motion vision system is no longer thought of as a purely feedforward sensory stream but is instead subject to behavioral-state modulation (1–3, 7, 34). Such modulation is consistent with the efficient coding hypothesis, which proposes that sensory circuits should match the bandwidth of the neural processing to that of expected stimuli, and therefore maximize the mutual information between their input and output (49–51). As the animal transitions from standing to walking to flight, the expected distribution of temporal frequencies of the visual stimuli shifts toward faster speeds, and it is consistent with efficient coding for the response function of the sensory system to show a corresponding shift to higher frequencies. Furthermore, this shift in encoding is predicted to occur early in the visual system, reducing the required dynamic range and preventing saturation of neurons within the circuit.

Despite experimental evidence and theoretical motivations for behavioral-state modulation of the visual system, the locations and mechanisms by which this modulation is implemented at the circuit level remain unclear. These questions are well posed in the ON motion pathway of *Drosophila*, where recent studies have characterized the responses of each of the major neuron types to visual stimuli, mapped out the anatomical and functional connectivity of neuron types, and described the effects of silencing each major neuron type on downstream neuronal activity and behavior (23, 27, 41). In this study, we found that most of the input neurons (Mi1, Tm3, and Mi4) have shifted baseline calcium activity during bouts of spontaneous activity, and all of the examined neurons (Mi1, Tm3, Mi4, Mi9, T4) have a significant calcium response to an air puff (Fig. 2). We also observed that bath application of the octopamine agonist CDM causes each of the examined neurons (Mi1, Tm3, Mi4, Mi9, T4) to respond

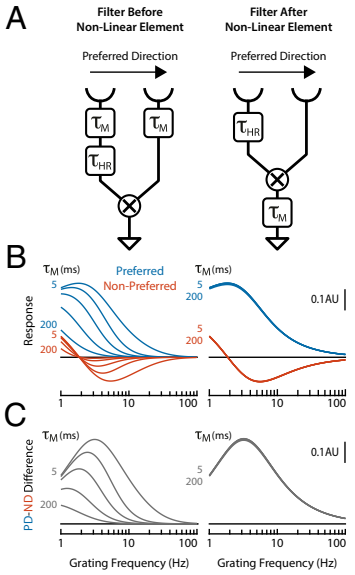

Fig. 7. Modulation of filter before, but not after, the correlation step of a motion detector alters speed tuning. (*A*) Schematic diagram of two computational models that implement variants of a Hassenstein–Reichardt correlator (52). In both models, light is transduced by photoreceptors (cup symbols), the signal from the leading photoreceptor passes through a low-pass filter (τ_{HR} = 50 ms), and the signals from both leading and trailing photoreceptor feed into a correlator ("X" symbol) that produces a directionally selective output. In the first model (*Left*), the circuit is modulated by two variable low-pass filters (τ_M) before nonlinear integration (i.e., the correlator). In the second model (*Right*), the circuit is modulated by a variable low-pass filter (τ_M) following nonlinear integration. (*B*) Tuning curves showing the response (in arbitrary units) of the two computational models to a sinusoidal grating (30° period). Responses are shown for gratings moving in both the preferred direction (PD) (in blue) and nonpreferred direction (ND) (in red), and for modulating filters with a range of time constants (τ_M = 5, 25, 50, 100, 200 ms). (*C*) Tuning curves showing the difference in the response of the computational models to gratings moving in the preferred vs. nonpreferred directions (PD – ND). Data are replotted from *B*.

more to higher-frequency visual stimuli (Fig. 4). These results suggest that much of the behavioral-state modulation of speed tuning in the ON motion pathway occurs early in this pathway, before the directionally selective T4 neurons. This modulatory signal is most likely carried by octopamine neurons that project from the central brain back into the optic lobes, and densely innervate the medulla, lobula, and lobula plate but not the lamina (14) (Fig. 1*B*). Therefore, it is likely that the modulation we see in the medulla interneurons of the ON pathway (Fig. 2) also represents one of the earliest points in the visual system where this modulation occurs.

To examine the consequences of speed-tuning changes at different points in the motion pathway, we constructed a simple computational model based on the Hassenstein–Reichardt (52) implementation of the EMD, the traditional model for insect motion detection. In the first variant of this model, low-pass filters (with a variable time constant representing the effect of behavioral-state modulation) were placed at each input, before the nonlinear integration. In the second variant, a low-pass filter was placed at the output, after the nonlinear integration (Fig. 7*A*). Since directional selectivity emerges in the dendrites of T4 neurons via a nonlinear integration of its inputs (23), the first variant simulates the case of modulation affecting the inputs to T4, while the second simulates modulation beyond the nonlinear dendritic integration in T4, which includes effects on the LPTCs. Varying the time constant for the low-pass filter substantially affected the speed tuning of EMD when the filters were placed before the nonlinear integration, while varying these time constants had no effect when the filters were placed after the nonlinear integration (Fig. 7 *B* and *C*). These results illustrate that behavioral-state modulation of the frequency response of the motion detector is only effective if it is implemented before the nonlinear integration that produces directional selectivity. This result is a necessary consequence of the computational architecture of the motion detector. The output of the nonlinear integration encodes a directionally selective signal in its time average, and additional downstream low-pass filters would not alter this time average. In contrast, temporal filtering before nonlinear integration would be expected to shape the final circuit output, which precisely matches our experimental findings, and is in agreement with a recent modeling study (41). This finding is also in agreement with previous studies on LPTCs that have inferred that behavioral-state and/or octopamine modulation is at least partially presynaptic to the LPTCs (3, 11, 34).

While behavioral-state modulation and octopamine neuromodulation were observed in several of the input neurons, Mi4 neurons appeared to be much more strongly affected than the other neurons we examined. We found that the baseline activity of Mi4 neurons increased dramatically during periods of spontaneous behavioral activity and following air puffs (Fig. 2). We also observed that the response of Mi4 neurons to moving gratings was substantially altered by spontaneous activity (Fig. 4*C*) and by treatment with the octopamine agonist CDM (Fig. 4*E*). Since these tuning curves were constructed from time-averaged responses, it is difficult to distinguish whether this represents a shift in baseline activity or a change in how the neurons encode the transient features of the visual stimulus. Nonetheless, these results do suggest that the behavioral state has a pronounced effect on the physiological properties of Mi4 neurons. Furthermore, we found that photoactivation of octopamine neurons produced the rapid onset of large and persistent calcium responses in Mi4 neurons (Fig. 5), providing further evidence that Mi4 neurons are subject to potent, direct octopamine neuromodulation. In addition, CDM treatment increased the magnitude of Mi4 responses to photoactivation of L5 neurons (Fig. 6), demonstrating that one of the effects of this octopamine neuromodulation is to increase the sensitivity of Mi4 neurons to its other inputs. This increased excitability may also explain the stronger responses of medulla interneurons to faster visual stimuli in active behavioral states.

Cumulatively, our results suggest that Mi4 neurons are likely to play a different role in the ON motion pathway when the animal is in a quiescent vs. active behavioral state. Previous studies indicated that directional selectivity of T4 neurons may involve a hybrid mechanism, involving features that resemble both the synergistic mechanism of a Hassenstein–Reichardt correlator (23, 24, 52–54) and the inhibitory veto mechanism of the Barlow–Levick detector (23, 53, 55). In this model, Mi4 neurons should contribute to the Barlow–Levick detector by providing inhibitory inputs to T4 neurons that are retinotopically offset from the excitatory inputs provided by Mi1 and Tm3 neurons (23, 27). In our previous study, we found that Mi4 neurons have low baseline activity and are relatively unresponsive to visual inputs when the animal is behaviorally quiescent (23), and in this study we found that Mi4 neurons have elevated baseline activity and increased excitability when the animal is behaviorally active. Taken together, these results appear to indicate that the computational architecture of the ON EMD may be fluid, behaving as a Hassenstein–Reichardt correlator when the animal is inactive, and adopting features of a Barlow–Levick detector when the animal is active. This may resolve a paradox from the previous study, where we observed that silencing Mi4 neurons produced significant changes in the behavioral response of flies to ON motion, but had only modest effects on the calcium responses of T4 neurons as measured in quiescent animals. Finally, there is an intriguing parallel between our findings and recent work in the mouse visual cortex, where inhibitory neurons were also found to track the behavioral

state of the mouse in the dark with much higher fidelity than excitatory pyramidal neurons (56). It seems likely that comparisons between organisms will continue to yield reciprocal insights as our understanding of these circuits develops.

Materials and Methods

Detailed methods are provided in *Supporting Information*. In brief, we used a two-photon microscope to image the in vivo calcium activity of *Drosophila* neurons labeled by Split-GAL4 lines following previously established methods for visual stimulus presentation and functional connectivity (22, 23). The spontaneous behavior of the flies was recorded during the imaging experiments. For behavioral experiments, the walking behavior of tethered female *Drosophila* was measured (23, 39) while visual stimuli were displayed (40).

ACKNOWLEDGMENTS. We thank Emily Willis for assistance with artwork; Gerry Rubin for supporting Aljoscha Nern; and Yoshi Aso, Heather Dionne, and Gerry Rubin for the gift of the Tdc2-GAL4 line. We also thank the Fly Functional Connectome Project for supporting the functional connectivity experiments and members of the M.B.R. laboratory for comments on the manuscript. This project was supported by Howard Hughes Medical Institute.

1. Chiappe ME, Seelig JD, Reiser MB, Jayaraman V (2010) Walking modulates speed sensitivity in *Drosophila* motion vision. *Curr Biol* 20:1470–1475.
2. Longden KD, Krapp HG (2009) State-dependent performance of optic-flow processing interneurons. *J Neurophysiol* 102:3606–3618.
3. Maimon G, Straw AD, Dickinson MH (2010) Active flight increases the gain of visual motion processing in *Drosophila*. *Nat Neurosci* 13:393–399.
4. Niell CM, Stryker MP (2010) Modulation of visual responses by behavioral state in mouse visual cortex. *Neuron* 65:472–479.
5. Krapp HG, Hengstenberg R (1996) Estimation of self-motion by optic flow processing in single visual interneurons. *Nature* 384:463–466.
6. Suver MP, Mamiya A, Dickinson MH (2012) Octopamine neurons mediate flight-induced modulation of visual processing in *Drosophila*. *Curr Biol* 22:2294–2302.
7. Jung SN, Borst A, Haag J (2011) Flight activity alters velocity tuning of fly motion-sensitive neurons. *J Neurosci* 31:9231–9237.
8. Cooper JR, Bloom FE, Roth RH (2003) *The Biochemical Basis of Neuropharmacology* (Oxford Univ Press, New York).
9. Adamo SA, Linn CE, Hoy RR (1995) The role of neurohormonal octopamine during "fight or flight" behaviour in the field cricket *Gryllus bimaculatus*. *J Exp Biol* 198: 1691–1700.
10. Longden KD, Krapp HG (2010) Octopaminergic modulation of temporal frequency coding in an identified optic flow-processing interneuron. *Front Syst Neurosci* 4:153.
11. Rien D, Kern R, Kurtz R (2012) Octopaminergic modulation of contrast gain adaptation in fly visual motion-sensitive neurons. *Eur J Neurosci* 36:3030–3039.
12. Tuthill JC, Nern A, Rubin GM, Reiser MB (2014) Wide-field feedback neurons dynamically tune early visual processing. *Neuron* 82:887–895.
13. van Breugel F, Suver MP, Dickinson MH (2014) Octopaminergic modulation of the visual flight speed regulator of *Drosophila*. *J Exp Biol* 217:1737–1744.
14. Busch S, Selcho M, Ito K, Tanimoto H (2009) A map of octopaminergic neurons in the *Drosophila* brain. *J Comp Neurol* 513:643–667.
15. Borst A (2014) Fly visual course control: Behaviour, algorithms and circuits. *Nat Rev Neurosci* 15:590–599.
16. Fischbach K-F, Dittrich A (1989) The optic lobe of *Drosophila melanogaster*. I. A Golgi analysis of wild-type structure. *Cell Tissue Res* 258:441–475.
17. Takemura SY, et al. (2013) A visual motion detection circuit suggested by *Drosophila* connectomics. *Nature* 500:175–181.
18. Behnia R, Clark DA, Carter AG, Clandinin TR, Desplan C (2014) Processing properties of ON and OFF pathways for *Drosophila* motion detection. *Nature* 512:427–430.
19. Clark DA, Bursztyn L, Horowitz MA, Schnitzer MJ, Clandinin TR (2011) Defining the computational structure of the motion detector in *Drosophila*. *Neuron* 70:1165–1177.
20. Joesch M, Schnell B, Raghu SV, Reiff DF, Borst A (2010) ON and OFF pathways in *Drosophila* motion vision. *Nature* 468:300–304.
21. Maisak MS, et al. (2013) A directional tuning map of *Drosophila* elementary motion detectors. *Nature* 500:212–216.
22. Strother JA, Nern A, Reiser MB (2014) Direct observation of ON and OFF pathways in the *Drosophila* visual system. *Curr Biol* 24:976–983.
23. Strother JA, et al. (2017) The emergence of directional selectivity in the visual motion pathway of *Drosophila*. *Neuron* 94:168–182.e10.
24. Fisher YE, Silies M, Clandinin TR (2015) Orientation selectivity sharpens motion detection in *Drosophila*. *Neuron* 88:390–402.
25. Serbe E, Meier M, Leonhardt A, Borst A (2016) Comprehensive characterization of the major presynaptic elements to the *Drosophila* OFF motion detector. *Neuron* 89: 829–841.
26. Buchner E (1976) Elementary movement detectors in an insect visual system. *Biol Cybern* 24:85–101.
27. Takemura SY, et al. (2017) The comprehensive connectome of a neural substrate for "ON" motion detection in *Drosophila*. *Elife* 6:e24394.
28. Luan H, Peabody NC, Vinson CR, White BH (2006) Refined spatial manipulation of neuronal function by combinatorial restriction of transgene expression. *Neuron* 52: 425–436.
29. Pfeiffer BD, et al. (2010) Refinement of tools for targeted gene expression in *Drosophila*. *Genetics* 186:735–755.
30. Lai SL, Lee T (2006) Genetic mosaic with dual binary transcriptional systems in *Drosophila*. *Nat Neurosci* 9:703–709.
31. Jenett A, et al. (2012) A GAL4-driver line resource for *Drosophila* neurobiology. *Cell Rep* 2:991–1001.
32. Chen TW, et al. (2013) Ultrasensitive fluorescent proteins for imaging neuronal activity. *Nature* 499:295–300.
33. Suver MP (2014) Octopamine neurons mediate flight-induced modulation of visual processing in Drosophila melanogaster. PhD thesis (California Institute of Technology, Pasadena, CA).
34. Fujiwara T, Cruz TL, Bohnslav JP, Chiappe ME (2017) A faithful internal representation of walking movements in the *Drosophila* visual system. *Nat Neurosci* 20:72–81.
35. Kim AJ, Fitzgerald JK, Maimon G (2015) Cellular evidence for efference copy in *Drosophila* visuomotor processing. *Nat Neurosci* 18:1247–1255.
36. Schnell B, Weir PT, Roth E, Fairhall AL, Dickinson MH (2014) Cellular mechanisms for integral feedback in visually guided behavior. *Proc Natl Acad Sci USA* 111:5700–5705.
37. Shinomiya K, et al. (2014) Candidate neural substrates for off-edge motion detection in *Drosophila*. *Curr Biol* 24:1062–1070.
38. Cole SH, et al. (2005) Two functional but noncomplementing *Drosophila* tyrosine decarboxylase genes: Distinct roles for neural tyramine and octopamine in female fertility. *J Biol Chem* 280:14948–14955.
39. Seelig JD, et al. (2010) Two-photon calcium imaging from head-fixed *Drosophila* during optomotor walking behavior. *Nat Methods* 7:535–540.
40. Reiser MB, Dickinson MH (2008) A modular display system for insect behavioral neuroscience. *J Neurosci Methods* 167:127–139.
41. Arenz A, Drews MS, Richter FG, Ammer G, Borst A (2017) The temporal tuning of the *Drosophila* motion detectors is determined by the dynamics of their input elements. *Curr Biol* 27:929–944.
42. Yao Z, Macara AM, Lelito KR, Minosyan TY, Shafer OT (2012) Analysis of functional neuronal connectivity in the *Drosophila* brain. *J Neurophysiol* 108:684–696.
43. Balfanz S, Strünker T, Frings S, Baumann A (2005) A family of octopamine [corrected] receptors that specifically induce cyclic AMP production or Ca^{2+} release in *Drosophila melanogaster*. *J Neurochem* 93:440–451, and erratum (2005) 94:1168.
44. Evans PD, Maqueira B (2005) Insect octopamine receptors: A new classification scheme based on studies of cloned *Drosophila* G-protein coupled receptors. *Invert Neurosci* 5:111–118.
45. Brand AH, Perrimon N (1993) Targeted gene expression as a means of altering cell fates and generating dominant phenotypes. *Development* 118:401–415.
46. Klapoetke NC, et al. (2014) Independent optical excitation of distinct neural populations. *Nat Methods* 11:338–346.
47. Tuthill JC, Nern A, Holtz SL, Rubin GM, Reiser MB (2013) Contributions of the 12 neuron classes in the fly lamina to motion vision. *Neuron* 79:128–140.
48. Hiripi L, Nagy L, Hollingworth RM (1999) In vitro and in vivo effects of formamidines in locust (*Locusta migratoria migratorioides*). *Acta Biol Hung* 50:81–87.
49. Atick JJ, Redlich AN (1990) Towards a theory of early visual processing. *Neural Comput* 2:308–320.
50. Barlow HB (1961) Possible principles underlying the transformations of sensory messages. *Sensory Communication*, ed Rosenblith WA (MIT Press, Cambridge, MA), pp 217–234.
51. Laughlin S (1981) A simple coding procedure enhances a neuron's information capacity. *Z Naturforsch C* 36:910–912.
52. Hassenstein VB, Reichardt W (1956) Systemtheoretische Analyse der Zeit-, Reihenfolgen- und Vorzeichenauswertung bei der Bewegungsperzeption des Rüsselkäfers Chlorophanus. *Z Naturforsch B* 11:513–524.
53. Haag J, Arenz A, Serbe E, Gabbiani F, Borst A (2016) Complementary mechanisms create direction selectivity in the fly. *Elife* 5:e17421.
54. Salazar-Gatzimas E, et al. (2016) Direct measurement of correlation responses in *Drosophila* elementary motion detectors reveals fast timescale tuning. *Neuron* 92: 227–239.
55. Barlow HB, Levick WR (1965) The mechanism of directionally selective units in rabbit's retina. *J Physiol* 178:477–504.
56. Pakan JM, et al. (2016) Behavioral-state modulation of inhibition is context-dependent and cell type specific in mouse visual cortex. *Elife* 5:e14985.
57. Nern A, Pfeiffer BD, Rubin GM (2015) Optimized tools for multicolor stochastic labeling reveal diverse stereotyped cell arrangements in the fly visual system. *Proc Natl Acad Sci USA* 112:E2967–E2976.
58. Iwai Y, et al. (1997) Axon patterning requires DN-cadherin, a novel neuronal adhesion receptor, in the *Drosophila* embryonic CNS. *Neuron* 19:77–89.
59. Wagh DA, et al. (2006) Bruchpilot, a protein with homology to ELKS/CAST, is required for structural integrity and function of synaptic active zones in *Drosophila*. *Neuron* 49:833–844.
60. von Reyn CR, et al. (2014) A spike-timing mechanism for action selection. *Nat Neurosci* 17:962–970.
61. Benjamini Y, Hochberg Y (1995) Controlling the false discovery rate—a practical and powerful approach to multiple testing. *J R Stat Soc Series B Stat Methodol* 57: 289–300.
62. Wilson RI, Turner GC, Laurent G (2004) Transformation of olfactory representations in the *Drosophila* antennal lobe. *Science* 303:366–370.
63. Demerec M (1965) *Biology of Drosophila* (Hafner, New York).